

The effect of dendritic topology on firing patterns in model neurons

Arjen van Ooyen¹, Jacob Duijnhouwer, Michiel W H Remme and Jaap van Pelt

Netherlands Institute for Brain Research, Graduate School Neurosciences Amsterdam, Meibergdreef 33, 1105 AZ Amsterdam, The Netherlands

Received 29 March 2002

Published 30 July 2002

Online at stacks.iop.org/Network/13/311

Abstract

Neuronal firing patterns are influenced by both membrane properties and dendritic morphology. Distinguishing two sources of morphological variability—metrics and topology—we investigate the extent to which model neurons that have the same metrical and membrane properties can still produce different firing patterns as a result of differences in dendritic topology. Within a set of dendritic trees that have the same number of terminal segments and the same total dendritic length, we show that firing frequency strongly correlates with topology as expressed by the mean dendritic path length. The effect of dendritic topology on firing frequency is bigger for trees with equal segment diameters than for trees whose segment diameters obey Rall's $\frac{3}{2}$ power law. If active dendritic channels are present, dendritic topology influences not only firing frequency but also type of firing (regular, bursting).

1. Introduction

Neurons are characterized by the shape of their axonal and dendritic arborizations. The soma and the dendritic arborizations receive and integrate incoming synaptic potentials and trigger the neuron to generate action potentials, which are transmitted to the neuron's target cells via its axonal arborizations. Dendritic morphology is assumed to play an important role in the generation of time-structured series of action potentials, through the way it influences both the integration of synaptic inputs and the spread of action potentials backward from soma to dendrites, as well as through influencing input conductance at the soma (for a review, see Segev and London (2000)).

Dendritic arborizations show an enormous diversity among and within neuron classes, both with respect to metrical characteristics (such as the total surface area of the dendritic

¹ Author to whom any correspondence should be addressed.

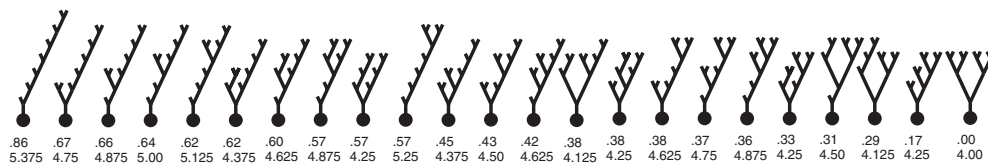


Figure 1. All the different degree 8 topologies. Upper index: tree asymmetry index. Lower index: normalized mean path length (each segment has length 1). For display purposes, some segments have been lengthened (in the simulations, all segments have the same length).

tree and the length and diameters of its segments) and with respect to topological structure (the connectivity pattern of the segments—as characterized, for example, by the topological asymmetry of the tree; see the methods section). The variation in topology can be accounted for by the growth process that generates the dendritic tree (e.g. Van Pelt and Uylings (1999)), and the mean asymmetry is often different for different neuron classes (e.g. Dityatev *et al* (1995), Van Pelt *et al* (1997, 2001), Van Pelt and Uylings (1999)). It is therefore important to know whether differences in dendritic topology, generated during growth, contribute to functional differences: i.e. to the neuron's electrophysiological properties (e.g. the type of firing patterns it can generate) and its role in neuronal signal processing.

In vivo and *in vitro* recordings of the electrical activity of neurons display a wide range of firing patterns. Experimental and theoretical studies show that differences in firing patterns between neurons can arise from differences in membrane properties, such as the types and densities of ion channels (Traub *et al* 1991, 1994, DeSchutter and Bower 1994, Jaffe *et al* 1994, Borg-Graham *et al* 1998). Several studies, however, have also emphasized the role of dendritic morphology (Bilkey and Schwartzkroin 1990, Mason and Larkman 1990, Pinsky and Rinzel 1994, Migliore *et al* 1995, Turner *et al* 1995, Mainen and Sejnowski 1996, Masukawa *et al* 1997, Sysmanzik *et al* 1999, Sheasby and Fohlmeister 1999, Washington *et al* 2000, Bastian and Nguyenkim 2001); see also Schubert *et al* (2001).

Mainen and Sejnowski (1996), for example, showed that multi-compartmental models of neocortical neurons that have the same channel densities and kinetics but differ in their dendritic shape and size can generate firing patterns ranging from regular spiking to bursting when stimulated at the soma with a fixed current injection. Reduced models consisting of only a dendritic and an axo-somatic compartment can give rise to the same spectrum of firing patterns, by varying the electrical resistance (coupling) between the two compartments and the ratio of the dendritic to axo-somatic surface area (Pinsky and Rinzel 1994, Mainen and Sejnowski 1996).

These model studies have shown that dendritic morphology has an influence on firing pattern, but they have not given insight into the possible separate roles of the two sources of morphological variability: metrics and topology (e.g. Van Pelt and Schierwagen (1994)). Stimulating at the soma and using a set of dendritic trees that have the same metrical and membrane properties but differ in their topological structure, we here investigate the extent to which dendritic topological structure can affect firing pattern.

Preliminary results of this study have been published in Duijnhouwer *et al* (2001).

2. Methods

To study the influence of dendritic topological structure on firing pattern, we used a set of neurons consisting of all the topologically different dendritic trees with eight terminal segments (i.e. the degree of the trees is 8; see figure 1). (For the basal dendrites of rat pyramidal neurons, for example, most topologically different tree types can actually be found for trees of a low

Table 1. Membrane properties. Conductances are in $\text{pS } \mu\text{m}^{-2}$. In addition, the dendrites contain an internal Ca^{2+} decay mechanism (which can be viewed as simplified buffering; see Destexhe *et al* (1993) and Mainen and Sejnowski (1996)). For both the axo-somatic compartment and the dendrites, the membrane capacitance (C_m) is $0.75 \mu\text{F cm}^{-2}$ and the axial resistance (R_a) is $150 \Omega \text{ cm}$. Further, the reversal potentials are $E_{\text{Na}} = 60 \text{ mV}$, $E_{\text{K}} = -90 \text{ mV}$, $E_{\text{Ca}} = 140 \text{ mV}$ and $E_{\text{leak}} = -70 \text{ mV}$.

Name of conductance	Axo-somatic	Dendrites
	active:	active:
Fast Na^+ conductance	$\bar{g}_{\text{Na}} = 3000$	$\bar{g}_{\text{Na}} = 15$
Fast non-inactivating K^+ conductance	$\bar{g}_{\text{Kv}} = 150$	
Slow voltage-dependent non-inactivating K^+ conductance		$\bar{g}_{\text{Km}} = 0.1$
Slow Ca^{2+} -activated K^+ conductance		$\bar{g}_{\text{KCa}} = 3$
High voltage-activated Ca^{2+} conductance		$\bar{g}_{\text{Ca}} = 0.3$
		passive:
Leak conductance		$\bar{g}_{\text{leak}} = 0.33$

degree—see Van Pelt and Uylings (1999).) All the segments in the trees (intermediate and terminal segments) have the same length, diameter ($5 \mu\text{m}$), and membrane properties, so that the trees differ only in the way the segments are connected, i.e. their topological structure. In addition to possessing a dendritic tree, all neurons have an axo-somatic compartment. Based on somatic surface area measurements of cortical pyramidal neurons (Uylings *et al* 1994), we took the diameter and length of the axo-somatic compartment equal to $20 \mu\text{m}$.

We also studied the situation where the diameters of the segments in the tree obey Rall's $\frac{3}{2}$ power law (Rall 1959), which says that the diameter of a parent segment, d_p , is related to the diameters of its daughter segments, d_1 and d_2 , as $d_p^e = d_1^e + d_2^e$, where the branch power parameter e is equal to $\frac{3}{2}$. In this situation, however, it is no longer possible to have a set of trees that differ only in topological structure, as different topologies will inevitably get different metrical properties. Based on two different ways of 'normalizing' for metrical properties, we implemented the power law in two ways. In the first implementation, we assumed equal terminal segment diameters ($1.25 \mu\text{m}$) across all topologies, based on the observation that the diameters of terminal segments show only a narrow range of values (Larkman 1991). This implies, however, that asymmetrical topologies get a higher total dendritic surface area than symmetrical topologies. In the second implementation of the power law, we kept the total dendritic surface area the same for all topologies. This implies that we had to assign different terminal segment diameters to each topology; for the total dendritic surface area and the total dendritic length we used, root segments become very thick (see section 3.2).

Ion channel types and densities were identical for all trees and were as in Mainen and Sejnowski's (1996) two-compartmental model (see table 1), except that we took \bar{g}_{Na} and \bar{g}_{Kv} ten times smaller, to compensate for the fact that we used a larger axo-somatic compartment than in Mainen and Sejnowski (1996). We studied both the situation where active channels were present in the dendrites and the situation where they were absent. Neurons were continuously stimulated at the axo-somatic compartment with a fixed current injection of 100 pA ; the resulting firing patterns were recorded from the axo-somatic compartment. Simulations were carried out in NEURON (Hines and Carnevale 1997).

Observed firing patterns were correlated with a number of morphometric parameters:

Topological asymmetry. A typical shape characteristic of a dendritic tree is the connectivity pattern of its segments (topological structure). A distinction is made between terminal segments

(ending in a tip) and intermediate segments (ending in a branch point) (see figure 1). To measure the topological asymmetry of a tree, the *tree asymmetry* index (Van Pelt *et al* 1992) was used. For a given tree α^n with n terminal segments, the tree asymmetry index A_t is defined as

$$A_t(\alpha^n) = \frac{1}{n-1} \sum_{j=1}^{n-1} A_p(r_j, s_j), \quad (1)$$

where $n-1$ is the number of bifurcation points, $A_p(r_j, s_j)$ is the partition asymmetry at the j th bifurcation point, and r_j and s_j are the number of terminal segments in the two subtrees emanating from the j th bifurcation point. At each of the $n-1$ bifurcation points, partition asymmetry indicates the relative difference in the number of bifurcation points, r_j-1 and s_j-1 , in the two subtrees:

$$A_p(r_j, s_j) = \frac{|r_j - s_j|}{r_j + s_j - 2} \quad (2)$$

for $r_j + s_j > 2$. By definition, $A_p(1, 1) = 0$.

The tree asymmetry index is 0 for a fully symmetrical tree and approaches 1 (for $n \rightarrow \infty$) for a fully asymmetrical tree. The tree asymmetry index has been shown to be a good descriptor of topological structure (Van Pelt *et al* 1992).

Mean path length. The mean path length is the sum of all dendritic path lengths measured from tip to soma divided by the number of terminal segments. Thus, for a given tree α^n with n terminal segments, the mean path length P_t is

$$P_t(\alpha^n) = \frac{1}{n} \sum_{j=1}^n P_j, \quad (3)$$

where P_j is the length of the dendritic path between the tip of the j th terminal segment and the soma.

Electrotonic transformed size. This dimensionless measure is based on the electrotonic transformation (Carnevale *et al* 1995), which defines electrotonic distance as the natural log of the voltage attenuation between two points on a neuron. The steady-state voltage attenuation over every segment in our degree 8 sample was computed using NEURON's impedance class. The electrotonic lengths can be summed, resulting in a total electrotonic transformed dendritic size.

3. Results

3.1. Comparison of the firing patterns between fully symmetrical and fully asymmetrical trees

To investigate whether topological asymmetry has an affect on firing pattern, we first consider fully symmetrical and fully asymmetrical trees.

First, trees with equal segment diameters and with active dendritic ion channels. For a total dendritic length of 2100 μm (as there are 15 segments in a degree 8 tree, the length of each segment is 2100/15 μm), the symmetrical and the asymmetrical tree display the same *type* of firing pattern—namely, regular and non-adapting—but the firing frequency is higher in the asymmetrical tree (figure 2). For a total dendritic length of 1150 μm , tree asymmetry influences also the type of firing (figure 2). The asymmetrical tree shows burst firing, whereas the symmetrical tree shows regular firing.

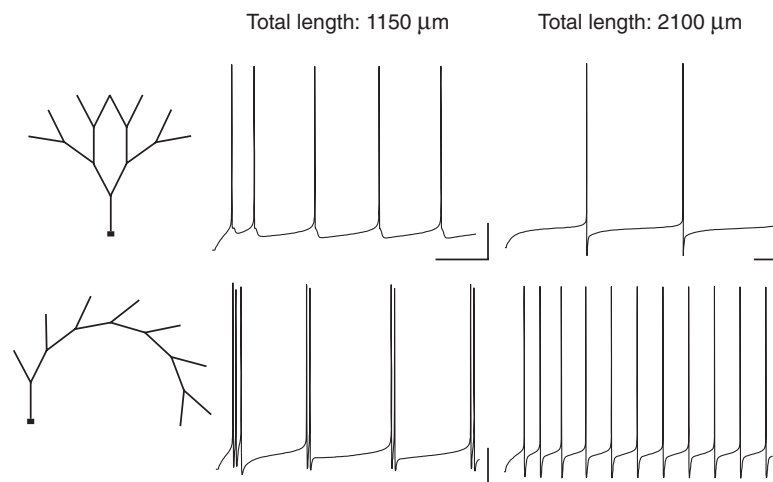


Figure 2. Firing patterns for a fully symmetrical and a fully asymmetrical tree. Active ion channels are present in the dendrites. All segments have the same diameter ($5 \mu\text{m}$). Both the type of firing and the frequency of firing can be influenced by dendritic topology. This is illustrated here for trees with total dendritic lengths of 1150 and 2100 μm . Scale bars: 100 ms, 25 mV.

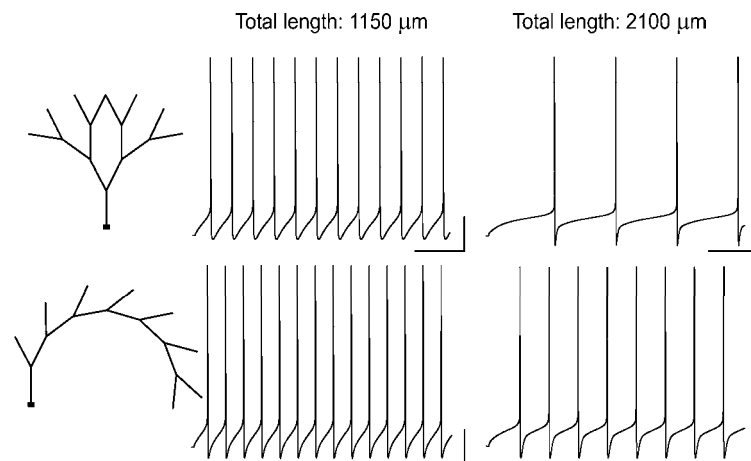


Figure 3. Firing patterns for a fully symmetrical and a fully asymmetrical tree. As figure 2, but without active ion channels in the dendrites. Under these conditions, only the frequency of firing can be influenced by dendritic topology. Scale bars: 100 ms, 25 mV.

In this model, the presence of active dendritic ion channels is necessary for bursting to occur (see also Pinsky and Rinzel (1994)); without active channels, only regular firing is possible, whereby, as in the case with active channels, the firing frequency for the asymmetrical tree is higher than for the symmetrical tree (figure 3).

If active dendritic channels are present, dendritic topology influences the type (and frequency) of firing also for trees whose segment diameters obey Rall's $\frac{3}{2}$ power law. The asymmetrical tree shows burst firing, whereas the symmetrical tree shows regular firing (figure 4).

The mechanism by which bursting is generated is as follows (see Mainen and Sejnowski (1996)). Once a spike is initiated in the soma, current leaks into the dendrites. The active ion

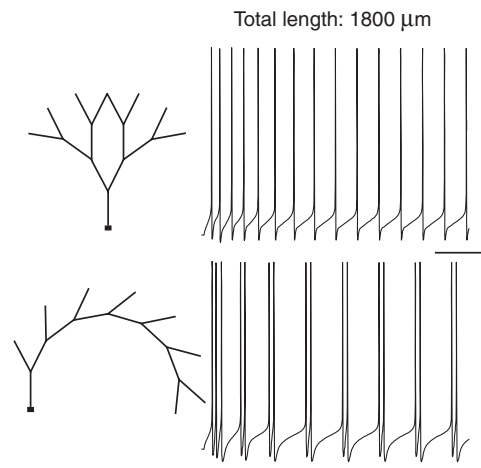


Figure 4. Firing patterns for a fully symmetrical and a fully asymmetrical tree. Active ion channels are present in the dendrites. The diameters of the segments in the trees obey Rall's $\frac{3}{2}$ power law (with equal terminal segment diameters of $1.25 \mu\text{m}$). The type (and frequency) of firing is influenced by dendritic topology, illustrated here for trees with a total dendritic length of $1800 \mu\text{m}$. Scale bars: 100 ms, 25 mV.

channels in the dendrites prolong this dendritic depolarization. After the soma has repolarized, current that returns from the dendrites into the soma produces an after-depolarization, which can give rise to another somatic spike. For both trees with equal segment diameters and trees whose segment diameters obey Rall's $\frac{3}{2}$ power law, this forward–backward interaction between the soma and dendritic tree is influenced by dendritic topology, as topology determines how much current leaks into the dendrites and how much current returns (see also section 3.3).

3.2. Correlations between morphometric parameters and firing frequency

To test whether in general tree asymmetry correlates with firing frequency, we recorded firing patterns from every degree 8 topology (see figure 1) and correlated firing frequency with the tree asymmetry index. We used a total dendritic length of $2150 \mu\text{m}$ because at this length each neuron shows the same type of firing, i.e. regular, non-adapting firing, so that differences in firing pattern reduce to differences in firing frequency. For trees with equal segment diameters, figure 5(A) shows that there is a weak positive correlation between firing frequency and tree asymmetry. Mean path length, however, proves to correlate much stronger with firing frequency (figure 5(B)). The correlation between firing frequency and mean path length also holds when there are no active ion channels in the dendrites (figure 5(C)). A third measure we correlated with firing rate is the electrotonic transformed size (see methods), which also shows a strong correlation (figure 5(D)).

It is important to realize that the correlation between firing frequency and mean path length holds within a set of trees that have the same degree and the same total dendritic length. Within such a set, the variability in mean path length is caused by topological variability. Increasing the total dendritic size of a tree, e.g. by increasing the lengths of all its segments, also increases the mean path length of the tree, but this results not in a higher but in a lower firing frequency (see section 3.4), because the input conductance is increased.

We also tested whether the correlation between firing frequency and mean path length holds if segment diameters obey Rall's $\frac{3}{2}$ power law (figure 6). In the first implementation of this

Equal diameters

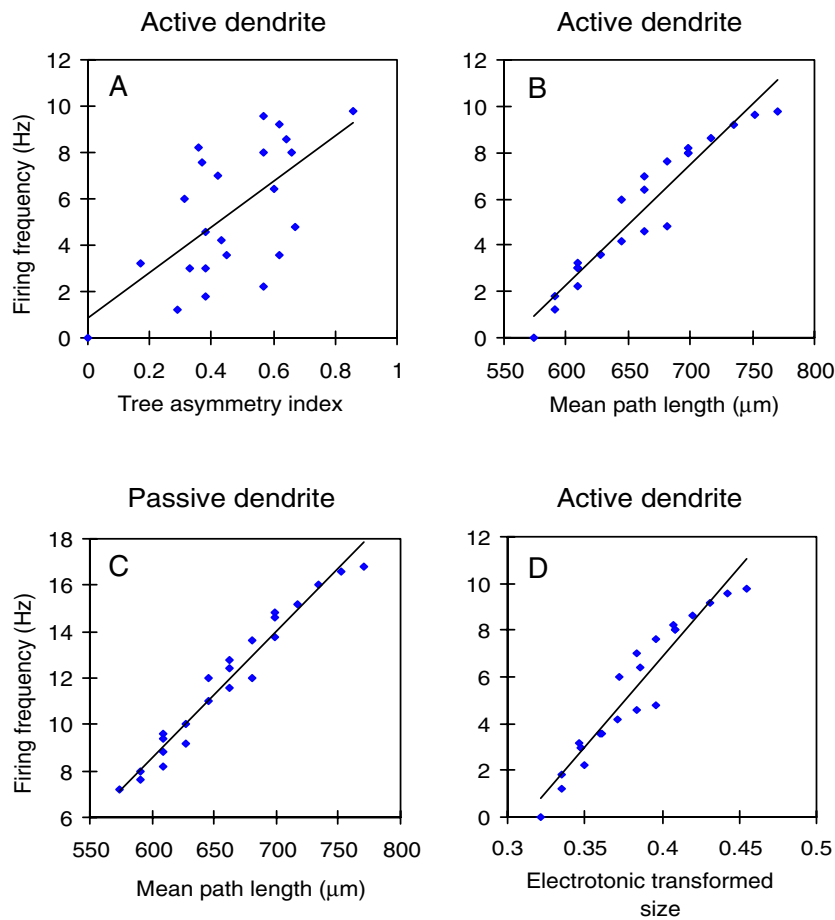


Figure 5. Correlation between firing frequency and various morphometric parameters. All segments of a tree have the same diameter ($5 \mu\text{m}$). Total dendritic length is $2150 \mu\text{m}$. Except for (C), all trees have active dendritic channels. Correlation between firing frequency and the tree asymmetry index (A), mean path length (B, C), and electrotonic transformed size (D). ((A): $R^2 = 0.40$, b (slope) = 9.8 ; (B): $R^2 = 0.92$, $b = 0.051$; (C): $R^2 = 0.96$, $b = 0.054$; (D): $R^2 = 0.92$, $b = 77$).

law—in which we assumed that all topologies have the same terminal segment diameter—we still find a positive correlation, but the variation in firing frequency becomes smaller (figure 6(A)), because under this implementation, asymmetrical topologies get a higher total dendritic surface area, which results in a higher input conductance and thus a lower firing frequency (see further section 3.3). In the second implementation of the power law, we kept the total dendritic surface area the same for all topologies (see methods). We set the total surface area at $2.75 \times 10^4 \mu\text{m}^2$, which is equivalent to the surface area of a tree with equal segment diameters of $5 \mu\text{m}$ and a total dendritic length of $1750 \mu\text{m}$. We used a total dendritic length of $1750 \mu\text{m}$, rather than $2150 \mu\text{m}$, to avoid very low firing frequencies. The firing frequencies become so low because under this implementation of the power law the root segments are very

Rall's 3/2 power law

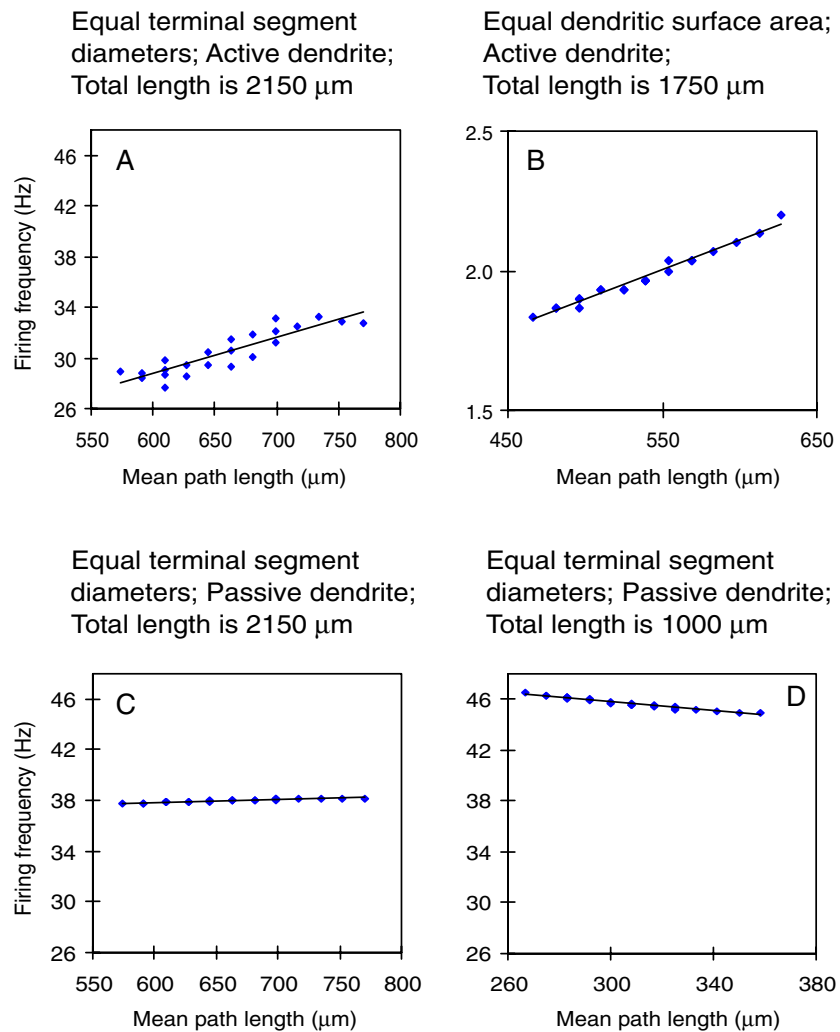


Figure 6. Correlation between firing frequency and mean path length when the diameters of the dendritic segments obey Rall's $\frac{3}{2}$ power law, implemented either with equal terminal segment diameters for all topologies (1.25 μm : (A), (C), and (D)) or with keeping the total dendritic surface area equal across different topologies (B) (see further section 3.2). In (A) and (B), the dendritic tree has active channels; in (C) and (D), it has not. The total dendritic length is 2150 μm in (A) and (C), 1750 μm in (B), and 1000 μm in (D). ((A): $R^2 = 0.80$, $b = 0.029$; (B): $R^2 = 0.98$, $b = 0.0021$; (C): $R^2 = 0.95$, $b = 0.0024$; (D): $R^2 = 0.97$, $b = -0.018$).

thick (10.7 μm in a fully asymmetrical tree, 12.8 μm in a fully symmetrical tree). Also with this implementation of the power law, we find a positive correlation between firing frequency and mean path length (figure 6(B)), although the variation in firing frequency is very small.

For a total dendritic length of 2150 μm , the positive correlation in trees that obey Rall's $\frac{3}{2}$ power law (with equal terminal segment diameters) still holds if there are no active dendritic

channels present (figure 6(C)), although now the variation in firing frequency becomes very small (see further section 3.3). For a much smaller total dendritic length, e.g. $1000 \mu\text{m}$, there is a negative correlation, again with a small variation in firing frequency (figure 6(D)).

3.3. Input conductance and dendritic topology

In this section, we further discuss the results described in sections 3.1 and 3.2. A large part of the results can be explained by considering the input conductance (at the soma) of a neuron with a passive dendritic tree and soma. Analytically, the input conductance in a passive dendritic tree can be determined using the formalism developed by Rall (1959) or, alternatively, from the current–voltage relation at the root segment using the formalism developed in Van Pelt (1992). The latter formalism gives a vector implementation of the Laplace-transformed cable equations, whereby the connectivity pattern of the segments in the tree is mapped directly onto the structure of the conductance matrix G (see also Van Pelt and Schierwagen (1994)). Using this formalism, and under the condition that all segments in the tree have the same diameter, one can show analytically that a symmetrical tree has a higher input conductance than an asymmetrical tree (see also figures 7(A), (E)). A higher input conductance means that more current leaks into the dendritic tree, and this results in a lowering of the firing frequency. Another way of understanding the difference in input conductance between a symmetrical and an asymmetrical tree is to consider that in a symmetrical tree the dendritic segments are, on average, located closer to the soma (i.e. are connected more ‘in parallel’) than in an asymmetrical tree (where the dendritic segments are connected more ‘in series’).

For equal diameters, there is a weak negative correlation between input conductance and tree asymmetry (figures 7(A), (E)), which is in agreement with the weak positive correlation found between firing frequency and tree asymmetry (figure 5(A)). For equal diameters, there is a much stronger negative correlation, however, between input conductance and mean path length (figures 7(B), (F)), which is in agreement with the strong positive correlation found between firing frequency and mean path length, both when the dendritic tree has active channels (figure 5(B)) and when it has not (figure 5(C)).

The mean path length measures how close, on average, the dendritic segments are to the soma; and the closer the segments are to the soma, the higher the input conductance. Although there is a correlation between tree asymmetry and mean path length (the highest mean path length is found in the fully asymmetrical tree, and the lowest mean path length in the fully symmetrical tree; see figure 8), firing frequency does not correlate so well with the tree asymmetry index, because, in the calculation of the tree asymmetry index, all partition asymmetries are weighted equally; i.e. the partition asymmetry associated with a bifurcation point far away from the soma contributes as much to the tree asymmetry as a partition asymmetry associated with a bifurcation point closer to the soma. For the effect on input conductance and thus firing frequency, however, asymmetries closer to the soma are more important than those further away.

In figures 5(B)–(D), the trees with a high firing frequency have in common that the partition associated with the bifurcation point closest to the soma is fully asymmetrical; i.e. at this bifurcation point, the tree is partitioned into two subtrees such that one has 1 and the other has $n - 1$ terminal segments. This again shows that partition asymmetries associated with bifurcations closer to the soma are relatively more important in influencing firing frequency.

For a total dendritic length of $2150 \mu\text{m}$, the positive correlation between firing frequency and mean path length still holds when segment diameters obey Rall’s $\frac{3}{2}$ power law (figures 6(A), (C)). In contrast to trees with equal segment diameters, the trees that obey Rall’s rule (with equal terminal segment diameters) show a *positive* correlation between input conductance and

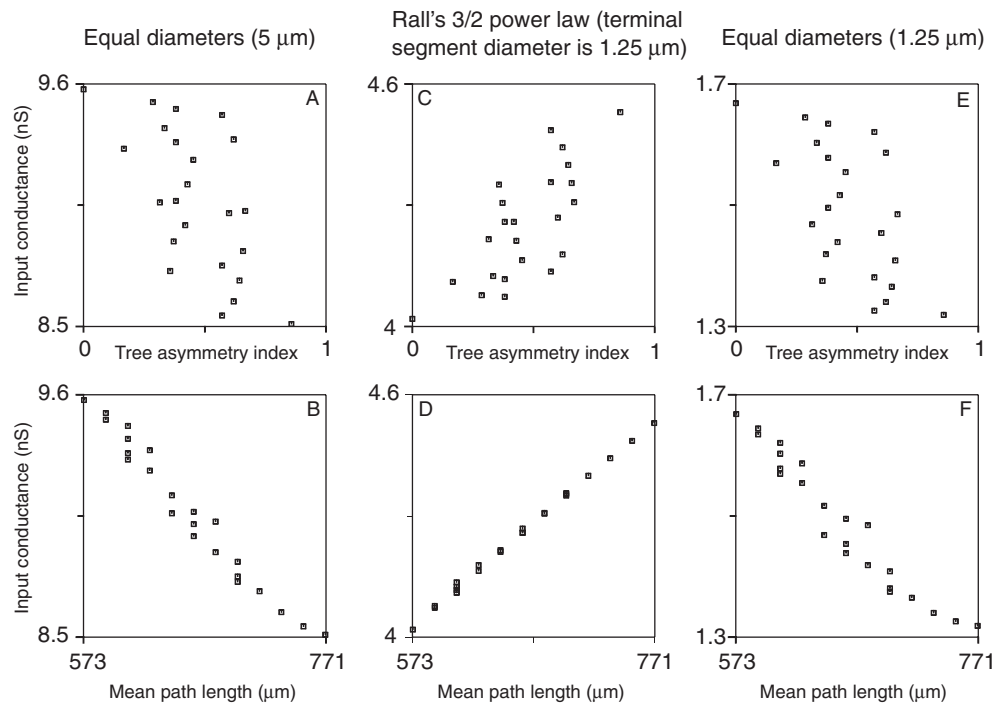


Figure 7. Correlation between input conductance and tree asymmetry (A, C, E) and between input conductance and mean path length (B, D, F) in degree 8 neurons with a passive dendritic tree and soma. Total dendritic length is $2150 \mu\text{m}$. Input conductance is determined analytically from the current–voltage relation at the root segment using the formalism developed in Van Pelt (1992). In (C) and (D), the diameters of the segments in the dendritic tree obey Rall's $\frac{3}{2}$ power law, whereby the diameters of the terminal segments are set at a fixed value of $1.25 \mu\text{m}$. In the other panels, all the segments in the tree have the same diameter: $5 \mu\text{m}$ (A, B) or $1.25 \mu\text{m}$ (E, F). For equal diameters, there is a negative correlation between input conductance and mean path length (and tree asymmetry); for segment diameters that obey Rall's power law, a positive correlation. Note that with Rall's power law, asymmetrical topologies (high mean path length) get a higher total dendritic surface area, resulting in a high input conductance. ((A): $R^2 = 0.39$, $b = -1.1$; (B): $R^2 = 0.97$, $b = -0.0059$; (C): $R^2 = 0.54$, $b = 0.54$; (D): $R^2 = 1.0$, $b = 0.0026$; (E): $R^2 = 0.37$, $b = -0.36$; (F): $R^2 = 0.94$, $b = -0.0020$; regression lines are not drawn).

mean path length (figure 7(D)), because implementing Rall's rule with equal terminal segment diameters gives asymmetrical topologies (and thus those with high mean path length) a higher total dendritic surface area than symmetrical trees, which increases the input conductance of asymmetrical trees. However, despite the fact that input conductance increases with increasing mean path length, we still find that firing frequency increases with increasing mean path length (although the variation in firing frequency is reduced). Note that the membrane capacitance of the dendritic tree has no effect on input conductance, since input conductance is measured under constant current conditions. Thus, interestingly, capacitance effects of the dendritic tree when the soma is generating action potentials—plus, in the case of figure 6(A), the effects of active channels in the dendritic tree—must be responsible for keeping up a positive correlation between firing frequency and mean path length. If there are no active channels in the dendritic tree and if the tree is much smaller (e.g. $1000 \mu\text{m}$), these effects are apparently not strong enough to keep a positive correlation between firing frequency and mean path length, and

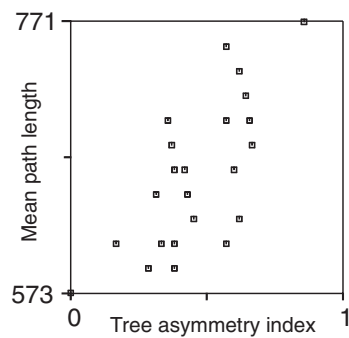


Figure 8. The correlation between mean path length and tree asymmetry index for the degree 8 topologies (total dendritic length is $2150 \mu\text{m}$). ($R^2 = 0.51$, $b = 206$).

we find a negative correlation instead (figure 6(D)) (although with a small variation in firing frequency).

3.4. The effect of total dendritic length on firing frequency

For neurons with a given dendritic topology, and with equal segment diameters, we studied the relationship between firing pattern and total dendritic length by increasing the length of the dendritic segments. As expected from the fact that a larger dendritic size gives a higher input conductance, the firing frequency drops with increasing total dendritic length (figure 9). At the same time, the differences in firing pattern between topologically different cells become more pronounced. For small trees, there are hardly any differences in firing frequency; the differences in firing frequency increase when the trees become bigger. At intermediate total dendritic lengths, a phase transition in firing behaviour occurs: cells start bursting, which explains the humps in the graph. This phase transition occurs for different topologies at different total dendritic lengths. When the total dendritic length is further increased, the cells revert to a regular firing pattern.

4. Conclusions and discussion

Using a set of model dendritic trees that have the same metrical and membrane properties but differ in topological structure has enabled us to study systematically the extent to which topology affects neuronal firing patterns. Using these models, we have shown that neurons that differ only in the topology of their dendritic tree can produce different firing patterns during somatic stimulation, even though they share the same types and densities of ion channels and have the same metrical properties. We have found the strongest effects of dendritic topology on firing frequency in dendritic trees with equal segment diameters and the smallest effects in passive dendritic trees that obey Rall's $\frac{3}{2}$ power law.

For dendritic trees with equal segment diameters, and within a set of trees that have the same degree and the same total dendritic length, there is a strong positive correlation between firing frequency and mean path length, and a weak positive correlation between firing frequency and tree asymmetry. These correlations are found both in the absence and in the presence of active dendritic channels. If active dendritic channels are present, dendritic topology influences not only firing frequency but also type of firing (regular, bursting). The positive correlation between firing frequency and mean path length is in agreement with the negative correlation

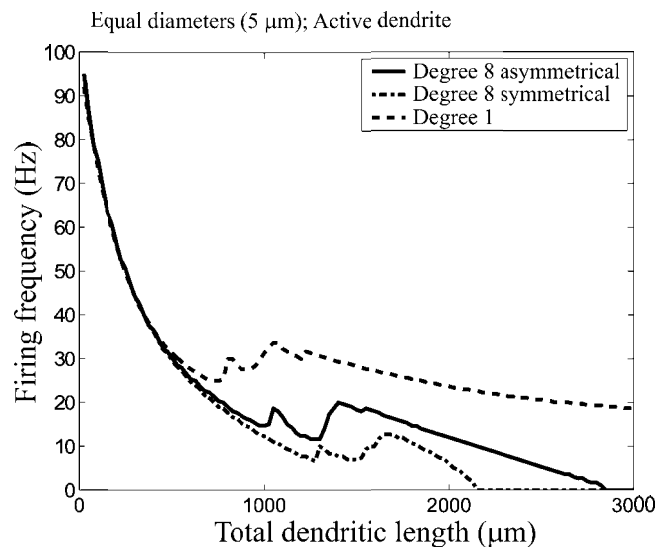


Figure 9. The influence of total dendritic length on the firing frequency of the fully symmetrical and asymmetrical degree 8 neurons, as well as of the degree 1 neuron. All the segments in a tree have the same diameter (5 μm) and there are active channels in the dendrites.

between input conductance and mean path length, as measured in trees without active channels in soma and dendrites.

If we want to obtain a better correlation between firing frequency and the tree asymmetry index, a weighted form of the tree asymmetry index may be considered in which partition asymmetries associated with bifurcation points closer to the soma are weighted more than partition asymmetries associated with bifurcation points farther away from the soma. Different weighting schemes are considered in Van Pelt *et al* (1992).

For dendritic trees whose segment diameters obey Rall's $\frac{3}{2}$ power law, we still find in most cases a positive correlation between firing frequency and mean path length, despite the fact that in these trees input conductance increases with increasing mean path length. As capacitance does not play a role in the measurement of input conductance, this implies that there must be important effects of the dendritic membrane capacitance (when the soma is generating action potentials) and of the active channels. There seems to be a balance between these effects and the (opposing) effect of the input conductance, because if the active channels in the dendrites are absent, we find in small dendritic trees a negative correlation between firing frequency and mean path length. Thus, in small, passive trees, the effects of input conductance seem to dominate the effects of dendritic capacitance.

As for dendritic trees with equal segment diameters, if active dendritic ion channels are present in trees whose segment diameters obey Rall's $\frac{3}{2}$ power law, dendritic topology influences not only firing frequency but also type of firing (regular, bursting).

Although we find a correlation between firing frequency and mean path length for dendritic trees that obey Rall's $\frac{3}{2}$ power law, the variation in firing frequency is small (especially for passive trees). Thus for these cells, changes in dendritic topology have only little effect on firing frequency—a property that may actually be desirable if the structure of the dendritic tree should not interfere with the cell's ability to measure input strength. We did not examine how the variation in firing frequency depends on the types and densities of ion channels, and it would be interesting to study whether other choices for these membrane properties could

result in a bigger variation in firing frequency. The type of firing (bursting, regular) may be more sensitive to dendritic topology than the frequency of firing; this is what we are currently investigating.

For dendritic trees with equal segment diameters, the variation in firing frequency as a result of differences in dendritic topology is larger. In biological neurons, the branch power parameter e (see methods) can be larger than $\frac{3}{2}$ (the larger e , the smaller the differences in segment diameters). For example, values of $e = 2$ were reported for guinea pig Purkinje cells (Rapp *et al* (1994), analysed in Van Pelt *et al* (2001)) and rat Purkinje cells and neocortical pyramidal neurons (Hillman 1979), and values of $1.5 < e < 2$ for rat visual cortex pyramidal neurons (Larkman *et al* 1992). On the basis of our results, we would predict that the larger e , the bigger the effect of dendritic topology on firing frequency.

Rather than trying to mimick existing experimental data on firing patterns, the goal of this study was to begin to explore the extent to which dendritic topology can affect firing pattern. We are not aware of any studies that have investigated whether or not topological variation is actually used in biological neurons to derive functional differences. Given the natural variation in dendritic topology (see introduction), and the results of our study, it would be interesting to look into dendritic topology as a possible factor contributing to functional differentiation.

A prediction of the model is that if we have a set of neurons with the same membrane properties (but with different metrical and topologies properties of their dendritic trees) and with the same firing frequency when stimulated at the soma, there may be a ‘trade-off’ between metrics and topology: in order to have the same firing frequency, asymmetrical trees should have a higher total dendritic length than symmetrical trees.

In order to test directly whether dendritic topology has an effect on firing pattern requires neurons with dendritic trees that differ only in their topology and that have as much as possible the same metrical and membrane properties. Using laser-scissor technology, it is in principle possible to manipulate (e.g. prune) dendritic morphology to create arbitrarily topologies (compare experiments by Goslin and Banker (1989) on transecting axons at various distances from the soma to study the development of polarity).

The electrical activity generated by a neuron with a particular dendritic morphology could subsequently change that morphology. Dendritic morphology is remarkably responsive to levels and patterns of neuronal activity (for reviews, see Van Ooyen (1994) and McAllister (2000)) and can change dramatically both during development and in adulthood (e.g. Purves *et al* (1986), Bailey and Kandel (1993), Wu *et al* (1999)). A major pathway by which activity affects morphology is through calcium signalling. Neuronal electrical activity and synaptic input affect calcium influx through voltage-gated calcium channels; intracellular calcium concentration, in turn, modulates the dynamics of the tubulin and the actin cytoskeleton, which control neurite elongation and branching (Forscher 1989, Sánchez *et al* 2000, Acebes and Ferrús 2000). Both the firing frequency and the type of firing are important in affecting neurite outgrowth. For example, Fields *et al* (1990) found that phasic stimulation is more effective in inhibiting neurite outgrowth than is stimulation with the same number of impulses at a constant frequency.

The precise dendritic topology may play a role in learning. Mel (1999) suggested models of development and learning that depend critically on computations in dendritic subregions (see also Mel *et al* (1998)).

Although stimulation of a neuron with a fixed current injection at the soma is used in many *in vitro* and *in vivo* studies and has also been used in many modelling studies—including this study—to explore the relationship between neuronal morphology and firing patterns, synaptic stimulation of the entire dendritic tree is a biologically much more realistic stimulation regime. It will therefore be important to test whether and how our results are affected when this stimulation regime is used. In addition to influencing the input conductance at the soma,

dendritic topology will then also influence the integration of synaptic inputs. The results of the present study will allow us to better distinguish between both these influences.

In Duijnhouwer *et al* (2001), it was shown that the results of Mainen and Sejnowski (1996)—obtained with somatic stimulation—on the relationship between type of spiking (regular firing or bursting) and dendritic morphology can be reproduced when synaptic stimulation of the dendritic tree is used.

Although we are aware that dendritic topology is just one factor contributing to the electrophysiological behaviour of the neuron, and that further research into the role of dendritic morphology is needed, we conclude from this study that neurons that have the same types and densities of ion channels and the same metrical properties can still produce different firing patterns (both with respect to firing frequency and type of firing) as a result of differences in dendritic topology.

Acknowledgments

We thank Dafna Fonds for help with the figures and an anonymous referee for useful suggestions.

References

- Acebes A and Ferrús A 2000 Cellular and molecular features of axon collaterals and dendrites *Trends Neurosci.* **23** 557–65
- Bailey C H and Kandel E R 1993 Structural changes accompanying memory storage *Ann. Rev. Physiol.* **55** 397–426
- Bastian J and Nguyenkim J 2001 Dendritic modulation of burst-like firing in sensory neurons *J. Neurophysiol.* **85** 10–22
- Bilkey D and Schwartzkroin P 1990 Variation in electrophysiology and morphology of hippocampal CA3 pyramidal cells *Brain Res.* **514** 77–83
- Borg-Graham L, Monier C and Fregnac Y 1998 Visual input evokes transient and strong shunting inhibition in visual cortical neurons *Nature* **393** 369–73
- Carnevale N T, Tsai K Y, Claiborne B J and Brown T H 1995 The electrotonic transformation: a tool for relating neuronal form to function *Advances in Neural Information Processing Systems* vol 7, ed G Tesoro, D S Touretzky and T K Leen (Cambridge, MA: MIT Press) pp 69–76
- DeSchutter E and Bower J 1994 An active membrane model of the cerebellar Purkinje cell I: simulation of current clamps in slice *J. Neurophys.* **71** 375–400
- Destexhe A, Babloyantz A and Sejnowski T J 1993 Ionic mechanisms for intrinsic slow oscillations in thalamic relay neurons *Biophys. J.* **65** 1538–52
- Dityatev A E, Chmykhova N M, Studer L, Karamian O A, Kozhanov V M and Clamann H P 1995 Comparison of the topology and growth rules of motoneuronal dendrites *J. Comp. Neurol.* **363** 505–16
- Duijnhouwer J, Remme M W H, Van Ooyen A and Van Pelt J 2001 Influence of dendritic morphology on firing patterns in model neurons *Neurocomputing* **38–40** 183–9
- Fields R D, Neale E A and Nelson P G 1990 Effects of patterned electrical activity on neurite outgrowth from mouse sensory neurons *J. Neurosci.* **10** 2950–64
- Forscher P 1989 Calcium and polyphosphoinositide control of cytoskeletal dynamics *Trends Neurosci.* **12** 468–74
- Goslin K and Banker G 1989 Experimental observations on the development of polarity by hippocampal neurons in culture *J. Cell Biol.* **108** 1507–16
- Hillman D E 1979 Neuronal shape parameters and substructures as a basis of neuronal form *The Neurosciences (4th Study Program)* ed F O Schmitt and F G Worden (Cambridge, MA: MIT Press) pp 477–98
- Hines M L and Carnevale N T 1997 The NEURON simulation environment *Neural Comput.* **9** 1179–209
- Jaffe D, Ross W, Lisman J, Lasser-Ross N, Miyakawa M and Johnston D 1994 A model for dendritic Ca²⁺ accumulation in hippocampal pyramidal neurons based on fluorescence imaging measurements *J. Neurophys.* **71** 1064–77
- Larkman A U 1991 Dendritic morphology of pyramidal neurones of the visual cortex of the rat: I. Branching patterns *J. Comp. Neurol.* **306** 307–19
- Larkman A U, Major G, Stratford K J and Jack J J B 1992 Dendritic morphology of pyramidal neurones of the visual cortex of the rat: IV. Electrical geometry *J. Comp. Neurol.* **323** 137–52
- Mainen Z and Sejnowski T 1996 Influence of dendritic structure on firing pattern in model neocortical neurons *Nature* **382** 363–6

- Mason A and Larkman A 1990 Correlations between morphology and electrophysiology of pyramidal neurons in slices of rat visual cortex I. Establishment of cell classes *J. Neurosci.* **5** 1407–14
- Masukawa L, Bernardo L and Prince D 1997 Variations in electrophysiological properties of hippocampal neurons in different subfields *Brain Res.* **242** 341–4
- McAllister A K 2000 Cellular and molecular mechanisms of dendrite growth *Cereb. Cortex* **10** 963–73
- Mel B W, Ruderman D L and Archie K A 1998 Translation-invariant orientation tuning in visual ‘complex’ cells could derive from intradendritic computations *J. Neurosci.* **17** 4325–34
- Mel B W 1999 Why have dendrites? A computational perspective *Dendrites* ed G Stuart, N Spruston and M Häusser (Oxford: Oxford University Press) pp 271–89
- Migliore M, Cook E, Jaffe D, Turner D and Johnston D 1995 Computer simulations of morphologically reconstructed CA3 hippocampal neurons *J. Neurophys.* **73** 1157–68
- Pinsky P F and Rinzel J 1994 Intrinsic and network rhythmogenesis in a reduced Traub model for CA3 hippocampal neurons *J. Comput. Neurosci.* **1** 39–60
- Purves D, Hadley R D and Voyvodic J T 1986 Dynamic changes in the dendritic geometry of individual neurons visualized over periods of up to three months in the superior cervical ganglion of living mice *J. Neurosci.* **6** 1051–60
- Rall W 1959 Branching dendritic trees and motoneuron membrane resistivity *Exp. Neurol.* **1** 491–527
- Rapp M, Segev I and Yarom Y 1994 Physiology, morphology and detailed passive models of guinea-pig cerebellar Purkinje cells *J. Physiol.* **474** 101–18
- Sánchez C, Díaz-Nido J and Avila J 2000 Phosphorylation of microtubule-associated protein 2 (MAP2) and its relevance for the regulation of the neuronal cytoskeleton function *Prog. Neurobiol.* **61** 133–68
- Schubert D, Staiger J F, Cho N, Kötter R, Zilles K and Luhmann H J 2001 Layer-specific and intracolumnar and transcolumnar functional connectivity of layer V pyramidal cells in rat barrel cortex *J. Neurosci.* **21** 3580–92
- Segev I and London M 2000 Untangling dendrites with quantitative models *Science* **290** 744–50
- Sheasby B W and Fohlmeister J F 1999 Impulse encoding across the dendritic morphologies of retinal ganglion cells *J. Neurophysiol.* **81** 1685–98
- Sysmanzik J, Ascoli G A, Krichmar J L and Washington S D 1999 Visual data mining of brain cell morphology and electrophysiology *Interface Stat. Comput. Sci.* **31** 445–9
- Traub R, Wong R, Miles R and Michelson H 1991 A model of a CA3 hippocampal neuron incorporating voltage-clamp data on intrinsic conductances *J. Neurophys.* **66** 79–95
- Traub R, Jeffreys J, Miles R, Whittington M and Toth K 1994 A branching dendritic model of a rodent CA3 pyramidal neurone *J. Neurophys.* **481** 635–50
- Turner D, Li X, Pyapali G, Ylinen A and Buzsáki G 1995 Morphometric and electrical properties of reconstructed hippocampal CA3 neurons recorded *in vivo* *J. Comp. Neurol.* **356** 580–94
- Uyilings H B M, Van Pelt J, Parnavelas J G and Ruiz-Marcos A 1994 Geometrical and topological characteristics in the dendritic development of cortical pyramidal and non-pyramidal neurons *The Self-Organizing Brain: From Growth Cones to Functional Networks (Progress in Brain Research vol 102)* ed J van Pelt, M A Corner, H B M Uyilings and F H Lopes da Silva (Amsterdam: Elsevier) pp 109–23
- Van Ooyen A 1994 Activity-dependent neural network development *Network: Comput. Neural Syst.* **5** 401–23
- Van Pelt J 1992 A simple vector implementation of the Laplace-transformed cable equations in passive dendritic trees *Biol. Cybern.* **68** 15–21
- Van Pelt J, Uyilings H B M, Verwer R W H, Pentney R J and Woldenberg M J 1992 Tree asymmetry—a sensitive and practical measure for binary topological trees *Bull. Math. Biol.* **54** 759–84
- Van Pelt J and Schierwagen A 1994 Electrotonic properties of passive dendritic trees—effect of dendritic topology *Prog. Brain Res.* **102** 127–49
- Van Pelt J, Dityatev A E and Uyilings H B M 1997 Natural variability in the number of dendritic segments: model-based inferences about branching during neurite outgrowth *J. Comp. Neurol.* **387** 325–40
- Van Pelt J and Uyilings H B M 1999 Natural variability in the geometry of dendritic branching patterns *Modeling in the Neurosciences, From Ionic Channels to Neural Networks* ed R R Poznanski (New York: Harwood Academic) pp 79–108
- Van Pelt J, Van Ooyen A and Uyilings H B M 2001 Modeling dendritic geometry and the development of nerve connections *Computational Neuroscience, Realistic Modeling for Experimentalists* ed E De Schutter (Boca Raton, FL: Chemical Rubber Company Press) pp 179–208
- Washington S D, Ascoli G A and Krichmar J L 2000 A statistical analysis of dendritic morphology’s effect on neuron electrophysiology of CA3 pyramidal cells *Neurocomp.* **32–3** 261–9
- Wu G Y, Zou D J, Rajan I and Cline H 1999 Dendritic dynamics *in vivo* change during neuronal maturation *J. Neurosci.* **19** 4472–83